

## Performance assessment and leakage analysis of feed water pre-heaters in natural gas-fired steam power plants

Gholamreza Ahmadi Sheikh Shabani<sup>a,\*</sup>, Mohammad Ameri<sup>a</sup>, Omidali Akbari<sup>b</sup>, Alireza Seifi<sup>b</sup>

<sup>a</sup>Mechanical and Energy Engineering Department, Shahid Beheshti University, Tehran, Iran;

<sup>b</sup>Young Researchers and Elite Club, Khomeinishahr Branch, Islamic Azad University, Isfahan, Iran

### Abstract

The performance of feed water pre-heaters (FWH) at a steam power plant with a capacity of 200 MW is evaluated in this paper. The main objective of this study is to investigate the behavior of these FWHs in various cases. The effect of leakage of condensates on the condenser was also studied in detail. To do this, each FWH was studied separately and also in groups (LP, HP and both groups). While some of the results are exclusive to the studied power plant, others can be generalized to similar power plants. The results show that although LPH-1 and LPH-2 have the lowest exergy efficiency, they have the greatest effect on the efficiency of the cycle. Whereas HPH-6 and LPH-4 have the highest heat exchange (31.3 and 21.73 MW), LPH-2 and LPH-1 deliver the greatest positive effect on energy efficiency (0.81% and 0.61/0%). Moreover, the results show the particular importance of preventing any leakage of heater condensate. In the event of leakage along the route to the condensate of heaters, the most negative effect will be due to the HP heaters: 20 kg/s leakage in the HPHs line will cause an increase in CO<sub>2</sub> production p.a. of roughly 10150 metric tons. Furthermore, energy efficiency and power produced will fall by 0.374% and 5.1 MW. In terms of the impact of leakages on the cooling tower, the study showed that LPH-1 and LPH-2 have the greatest effect. The effects of LP and HP FWHs on the energy efficiency of the cycle were 2.53% and 0.82%.

**Keywords:** Thermal power plants; Rankine cycle; Efficiency improvement; Feed water heater; Technical analysis; External leakage

### 1. Introduction

The issue of energy is becoming more important every day. Perhaps the environmental aspects can be considered as the most important reason for focusing on reducing energy consumption. The cost of electricity generation from renewable energy sources is currently higher than fossil fuel power plants [1]. Currently, Rankine cycle power plants have the largest share of power generation in the world [2]. These cycles are used in steam power plants (SPP) (fossil fuel types), combined cycle power plants (CCPP) and nuclear power plants [3]. Many studies have been carried out to increase the efficiency and performance of these types of power plants. Considering that power plants based on this cycle will be used for at least the next few decades (especially nuclear power plants and CCPP), research will continue with a view to increasing their efficiency. In developing countries, it is expected that at least in the next few decades,

fossil fuels will be the major source of electricity production [1]. In Iran, the same trend is predicted [4]. The Rankine cycle is also used in some solar thermal power plants to convert solar energy captured in solar collectors to power. There, the solar field acts as the energy source (instead of a boiler) and the cycle may include feed water.

In order to compare SC power plants with CCPPs, it is clear that GTCC power plants enjoy higher efficiency than SC power plants. This is because of the optimal use of fuel energy in the Brayton cycle (gas turbine) and the Rankine cycle (steam part). Many studies have been conducted into converting the simple cycle of MSPP into CCPP (repowering the cycle) [5–14], evaluating various methods of repowering. Technical and economic constraints apply to repowering existing steam power plants into CCPPs.

Rankine cycle efficiency can be improved by using FWHs [3]. Although the source of FW pre-heating is extracted steam from the turbine (which could generate power in the turbine), pre-heating has a greater effect on cycle efficiency and performance. In the newest Rankine cycle power plants, up to eight FWHs are used [3].

\*Corresponding author

Email address: gholamreza.ahmadi@iaukhsh.ac.ir (Gholamreza Ahmadi Sheikh Shabani)

## 2. Literature review

Many papers study feed water pre-heaters in Rankine cycles power plants. Some papers analyzed overall cycle performance while others studied internal heat transfer processes. The effect of leakage (internal or external) on the heat exchanger is also important and a summary of papers in this regard is presented.

Varma and Srinivas [15] studied optimum pressure and flashing factor in a CHP plant in India. To increase the system's efficiency, they used the waste heat of a cement factory to pre-heat the FW. Their results ultimately showed that waste heat recovery can be increased by reducing the temperature ratio from 0.5 to 0.25. Pourshaghaghay [16] studied the effect of pressure and the percentage of steam entering the FWs of a steam power plant. They chose the efficiency of the Rankine cycle as the objective function, while nonlinear constraints were used for optimization. Finally, calculations and optimization revealed that the optimum pressure for each FWs differed slightly from the existing values.

Moghadassi et al. [17] calculated the working conditions of a heat recovery cycle with an open FW and sought to maximize the output power of the cycle. They used a genetic algorithm for optimization and a neural network to find the thermodynamic properties of water at cyclic points. Boiler pressure was 5 MPa in the cycle studied.

Farhad et al. [18] used exergy and pinch analysis to reduce the irreversibility of FWs at four operating power plants. The boiler pressure of these power plants was subcritical. Akolekara et al. [19] found the best reheater pressure and FWs in a power plant. They studied boilers with pressures up to 22 MPa. Jiping et al. [20] investigated the effects of partial load of a coal-fired power plant on FWs. Moving away from design conditions can reduce the performance of the pre-heaters. They assessed a super-critical power plant with a capacity of 660 MW and concluded that the use of an ejector pump system which uses main line steam could significantly increase the performance of the pre-heaters.

Antar and Zubair [21] studied the performance of a power plant's FWs. By examining all parts of a heater – including the desuperheater section, condenser and sub-cooler parts – they found that the mass flow rate of steam and heat transfer coefficient have a great influence on the performance of the heaters. By examining the heat transfer process and its change over time, they concluded that 3 years after the installation of these heaters, the heat transfer rate will decrease by 2.7%.

Xu et al. [22] studied the effect of water level (condensate) inside the FWs on their performance. They first developed a mathematical model to estimate the parameters of the heater using dimensional parameters. A high-pressure (HP) heater from a 330 MW coal-fired power plant was used and they examined the effects of fluid level on the performance of different parts such as the drain cooler. They showed that this model can be used to predict the performance of the operating heaters to find the best performance mode.

Álvarez-Fernández et al. [23] performed thermodynamic

analysis of closed FWs of a nuclear power plant and proposed a model for thermal analysis of heaters when their input steam is in saturation mode. A method for remote evaluation of heater performance was proposed, as heaters in nuclear power stations contain radioactive materials.

Espatolero et al. [24] introduced strategies to improve efficiency while designing a network of FWs in supercritical coal-fired power plants. Their results showed that the overall efficiency of the cycle can be increased by up to 0.7%. Moreover, a 1.3% reduction in CO<sub>2</sub> production was achieved.

Hossienalipour et al. [25] developed a model for assessing the effect of water level on the cooling rate of the drain cooler in vertical HP FWs. They introduced a mathematical model for evaluating the performance of a three-part HP pre-heater. Results showed that the water level inside the heater has a great influence on its performance.

In this paper, we analyze the performance of FWs of a steam power plant as a case study. The proposed power plant has 4 LP heaters and 3 HP heaters and an open heater (Deaerator). We first simulated the cycle using Cycle Tempo software and compare it with the design and operation results. After ensuring the validity of the results, we examined possible changes to cycle performance. To analyze these heaters, while taking into account different working conditions that occur in the power plant, we examined the effects of these changes on the overall performance of the cycle. The effect of lowering the performance of the heater and taking each heater out of service were considered. Also, due to the impact of the leakage of condensate forming in the heaters, this issue was also studied in detail. The introduction of leaked water into the condenser increases the thermal load and as a result, reduces the condensed vacuum and ultimately reduces the production power or increases the heat rate (HR) of the cycle [2]. Previous studies about the declining performance of heaters over time are presented. This applies to almost all Rankine cycle power plants [21]. This depends on the chemical composition of water and the material of the heater [26]. Furthermore, other parameters like fuel flexibility, operational flexibility and decreasing environmental undesirables (such as CO<sub>2</sub>) are very important [27, 28], although fuel flexibility is not considered in this paper.

## 3. Description of the Power Plant Cycle

Montazeri Steam Power Plant (MSPP) consists of 8 units of 200 MW [29]. The main fuel of the boilers is mazut, but natural gas and diesel fuels are also used. Currently, due to limitations imposed by the Iranian Environment Organization, only natural gas is used [30].

Fig. 1 shows the main water and steam flow diagram of this power plant. In this cycle, in order to increase efficiency and maintain other relevant benefits, 7 closed FWs and one deaerator are used. In Table 1, the thermodynamic characteristics of the various points of the cycle are presented. Some general characteristics of the cycle are presented in Table 2. A brief description is given of the process of conveying water from the condenser to the boiler as well as the

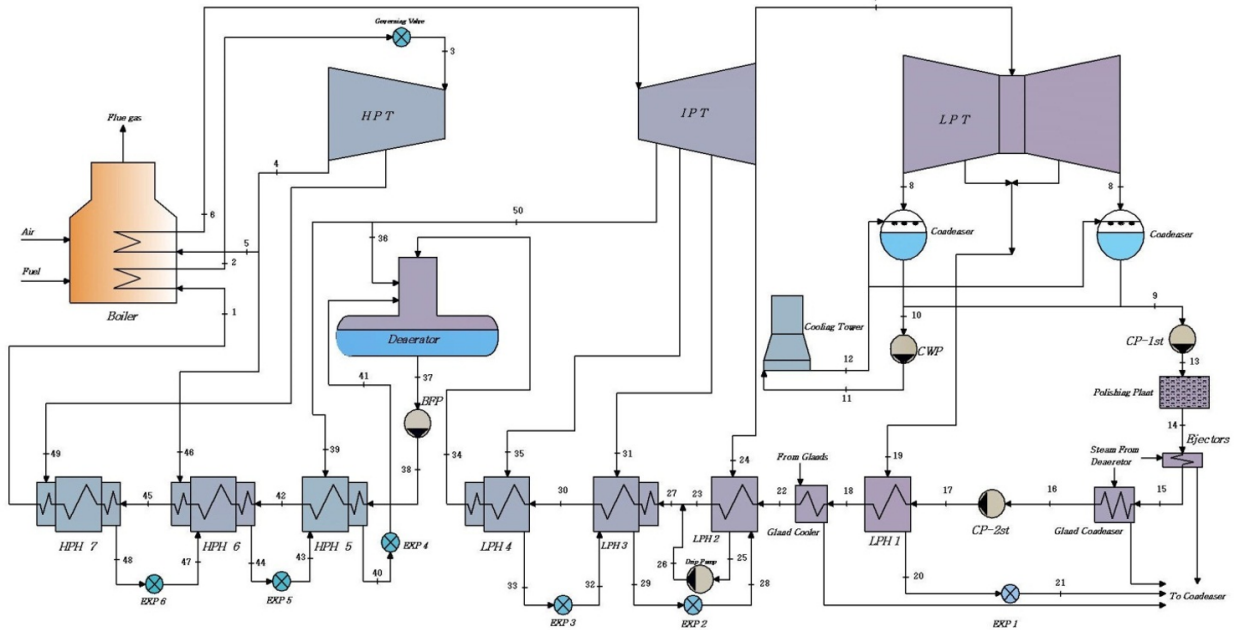


Figure 1: Schematic diagram of the reference power plant [27]

temperature range. The outlet water from the condenser at 47°C is pressurized by the first stage pumps to about 8 bar. In order to control water quality, a polishing plant is installed at this point. The water is filtered in two steps through the cationic filters and the mix-bed. The equipment requiring the low temperature FW (for cooling purposes) include: the main ejectors for producing condenser vacuum and keeping it fixed (two pieces of apparatus) and a Gland Condenser (GC). For this reason, the output water from the PP passes through this equipment. In order to compensate for the drop in pressure, the second stage pumps in this section increase the pressure of the water to about 21 bars. The outlet water from this pump(s) enters LP heater No. 1. After that, the water enters the Gland Steam Cooler (GSC). The gland steam from the turbines (HPT & IPT) is condensed in this heat exchanger. FW passes through LPHs 2, 3 and 4 upon exiting the GSC. Before entering the boiler feed pumps (BFP), FW enters the deaerator. The process of degassing is carried out in the deaerator, during the heating of the FW (max. 15 to 20°C). The purpose of degassing is also to remove some intrusive substances and insoluble oxygen from the FW. FW enters the deaerator at a temperature of 157°C. The FW enters HPHs (5, 6 and 7) after BFPs. Finally, the FW enters the steam generator at a temperature of 247°C and pressure of 172 bar.

#### 4. Governing Equations in Thermodynamic Modeling

The first law of thermodynamics, exergy balance and law of conservation of mass are used in a control volume. The first law of thermodynamics is [31]:

$$\sum \dot{m}_i (h_i + \frac{v_i^2}{2} + gz_i) + \dot{Q} = \sum \dot{m}_o (h_o + \frac{v_o^2}{2} + gz_o) + \dot{W} \quad (1)$$

The exergy balance equation [31]:

$$\sum \left(1 - \frac{T_0}{T}\right) \dot{Q} + \sum (\dot{m}_i \psi_i) = \sum \psi + \sum (\dot{m}_o \psi_o) + \dot{I}_{des} \quad (2)$$

The rate of irreversibility production [31]:

$$\dot{I}_{des} = \left( \sum \dot{m}_i \psi_i - \sum \dot{m}_o \psi_o \right) + \sum \left(1 - \frac{T_0}{T}\right) \dot{Q} - \dot{W} \quad (3)$$

To calculate the exergy for single-phase flows such as water or steam flow [2]:

$$\psi = (h - h_o) - T_o(s - s_o) \quad (4)$$

The transferred exergy by heat:

$$\psi_Q = Q \left(1 - \frac{T_o}{T}\right) \quad (5)$$

The energy efficiency ( $\eta_1$ ) and exergy efficiency ( $\eta_2$ ) are calculated using the following equations:

$$\eta_1 = \frac{P_{gen,net}}{\dot{Q}_f} = \frac{P_{gen,net}}{\dot{m}_f \times LHV} \quad (6)$$

$$\eta_2 = \frac{P_{gen,net}}{Ex_f} = \frac{P_{gen,net}}{\dot{m}_f \times LHV \times \xi} \quad (7)$$

Where  $\xi$  depends on the chemical composition of consumption fuel and it is expressed in numerous experimental values in different references. For usual gaseous fuels, one may write [32]:

Table 1: Thermodynamic properties of points in the cycle (According to Fig. 1)

Node	T, K	P, MPa	m, kg/s	H, kJ/kg	s, kJ/kg K	$\psi$ , kJ/kg	Ex, MW
1	519	17	179.4	1066	2.725	258.3	46337
2	813.1	13	179.4	3444	6.574	1488	266977
3	813.1	9.9	179.4	3477	6.731	1475	264535
4	606.2	2.802	171.4	3079	6.714	1082	185451
5	606.2	2.802	161.5	3079	6.714	1082	174696
6	813.1	2.42	161.5	3552	7.452	1335	215551
7	450	0.127	137.8	2828	7.622	559.8	77137
8	318.2	0.017	133.1	188.4	0.6385	2.607	346.9
9	308.2	0.075	137.8	146.7	0.5049	0.6649	91.62
10	318.2	0.075	6944	188.5	0.6385	2.665	18505
11	318.2	0.215	6944	188.6	0.6386	2.808	19494
12	308.2	0.08	6944	146.7	0.5051	0.6713	4661
13	308.6	0.9	137.8	149.5	0.5114	1.561	215.1
14	308.6	0.51	137.8	149.1	0.5116	1.17	161.3
15	310.2	0.420	137.8	155.3	0.5319	1.308	180.3
16	312.2	0.31	137.8	163.6	0.5588	1.547	213.2
17	312.3	1.95	137.8	165.9	0.5608	3.228	444.8
18	322.5	1.73	137.8	207.9	0.6939	5.564	766.7
19	344.1	0.043	4.72	297.2	0.9671	13.42	63.35
20	329.1	0.035	4.72	234.4	0.7807	6.245	29.48
21	329.1	0.017	4.72	234.4	0.7807	6.227	29.39
22	325.1	1.6	137.8	219.1	0.7288	6.327	871.9
23	357.7	1.4	137.8	354.9	1.128	23.27	3207
24	443.2	0.13	5.5	2814	7.58	558.4	3071
25	378.5	0.13	17.79	441.5	1.366	38.63	687.1
26	379.3	1.45	17.79	445.8	1.374	40.64	723
27	360.1	1.4	155.6	365.2	1.156	25.02	3893
28	386.3	0.13	12.29	2697	7.298	525.9	6462
29	385.3	0.265	12.29	470.3	1.442	45.06	553.8
30	384.5	1.2	155.6	467.6	1.432	45.22	7035
31	532.3	0.265	5.12	2987	7.61	722.6	3700
32	430.5	0.265	7.169	2779	7.177	644	4617
33	430.5	0.598	7.169	664.4	1.917	97.42	698.4
34	432.1	0.9	155.6	671.5	1.933	99.85	15535
35	644.2	0.598	7.169	3209	7.617	942.9	6760
36	720.3	1.248	1.8	3361	7.504	1129	2032
37	438.3	0.77	179.4	698.3	1.995	108.2	19410
38	440	15.5	179.4	715.5	1.989	127	22780
39	721.2	1.123	4.07	3365	7.557	1116	4543
40	459	1.123	22.01	2784	6.551	835.8	18398
41	459	0.75	22.01	2809	6.78	792.3	17439
42	454.5	18.00	179.4	777.8	2.13	147.4	26439
43	511.6	1.123	17.94	2911	6.813	884.5	15868
44	511.6	2.802	17.94	2830	6.265	966.5	17340
45	489.3	17.5	179.4	930.7	2.455	203.3	36472
46	603.6	2.802	9.94	3073	6.703	1079	10724
47	507.6	2.802	8	2817	6.24	961.3	7690
48	507.6	4.151	8	1011	2.649	266.2	1810
49	679.2	4.151	8	3268	6.832	1235	9882
50	720.3	1.248	5.87	3361	7.504	1129	6625

$$\begin{aligned}\xi_{CH4} &= 1.06 \\ \xi_{H2} &= 0.985\end{aligned}\quad (8)$$

For fuel with the formula  $C_xH_y$ , the following experimental equation is used to calculate  $\xi$  [32]:

$$\xi = 1.033 + 0.0169\frac{y}{x} - \frac{0.0698}{x}\quad (9)$$

The functional and universal exergy efficiencies ( $\eta_{2,f}$  and  $\eta_{2,u}$ ) of heat exchangers are calculated using following equations [33]:

$$\eta_{2,f} = \frac{Ex_{p,o} - Ex_{p,i}}{Ex_{s,i} - Ex_{s,o}}\quad (10)$$

$$\eta_{2,u} = \frac{\sum Ex_o + \sum \dot{I}}{\sum Ex_i}\quad (11)$$

Table 2: Operating conditions of the power plant [29]

Operating conditions	value	unit
Power produced	200	MW
Internal Power consumption	14	MW
Volumetric flow rate of fuel (Natural gas)	$54 \cdot 10^3$	Nm <sup>3</sup> /h
Volumetric flow rate of inlet air to burners	$9.6 \cdot 10^5$	Nm <sup>3</sup> /h
Heat rate	10448.6	kJ/kWh
Rate of CO <sub>2</sub> production	0.514	Kg/kWh
Stem flow rate, main line	186.1	kg/s
Steam pressure, main line	130	bar
Steam temperature, main line and reheat	540	°C
Water temperature, to boiler	247	°C
Stack gas temperature	160	°C
Number of induced and forced draft fans	2	-
Number of burners	12	-
Number of LPHs-HPHs	4–3	-

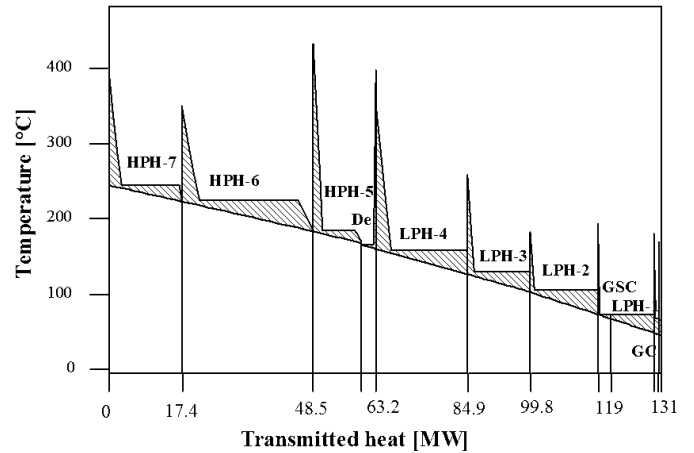


Figure 2: The Q-T diagram of FW heating process in the cycle

where subscripts p and s refer to primary and secondary paths in a heat exchanger. For FWs, the FW line is primary line and the steam line is secondary line.

Heat rate (HR) of a Rankine cycle is defined as the amount of required heat to produced work. It is inversely proportional to thermal efficiency [34]:

$$HR_{RC} = \frac{\dot{m}_f LHV_f}{P_{gen,net}} \cdot 3600\quad (12)$$

## 5. Results and Discussion

In order to investigate the effect of the presence of FWs (low pressure and high pressure), the cycle of the power plant is simulated in Cycle Tempo software [35]. For optimal results, technical information and instructions in the technical archive of the power plant were used [17]. Simulation results were compared with the heat balance parameters and manufacturer's performance diagrams, which showed good agreement between results [9].

In Fig. 2, the Q-T diagram of the pre-heating process of FW before entering the boiler is depicted, showing how FW temperature changes. In the process of heat exchange between FW and steam, only heating in the liquid phase is performed on the FW path. However, on the steam side, given that

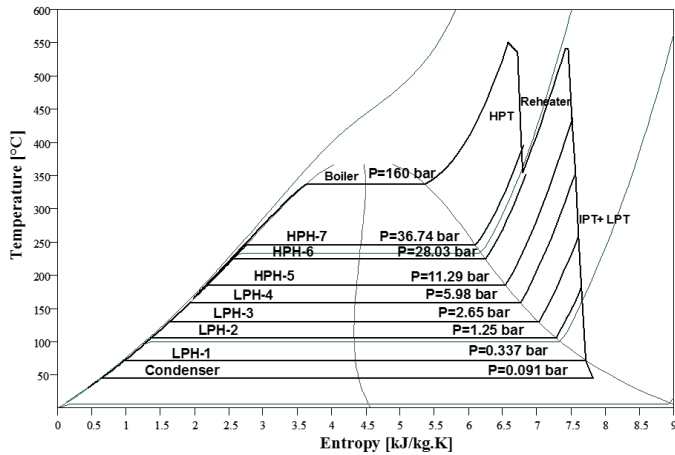


Figure 3: T-S diagram of the cycle

the steam enters in superheated form and exits as a compressed liquid, three processes occur: desuperheating, condensing and subcooling. In all heaters, there is a condensing section, but the presence of the other two (desuperheating and subcooling) depends on the temperature difference between water and steam as well as the design conditions of the heater. In general, when the heater inlet temperature is higher, the desuperheater and subcooler become more necessary [3]. In Fig. 2 it is seen that the total transferred heat to FW is about 134 MW.

In Table 3, some thermodynamic characteristics of FW and steam paths are observed for all heaters. The table includes inlet and exit temperature of the FW, temperature and pressure of steam, pressure drop of FW, exchanged heat, difference in the temperature of the FW in the heater and the presence or absence of a desuperheater and subcooler (also called steam cooler and drain cooler). A steam cooler is added to this type of heat exchanger to minimize the temperature difference between the two fluids in the heat exchange process [3] thereby reducing the thermal stress and exergy losses [32]. A drain cooler is added to overcool the outlet condensate of the heater and maximize the use of energy from the condensed steam. This reduces the probability of reaching a two-phase mode in the pipeline and the pump (drip pump) while lowering the heat of the outlet condensate. The output condensate from each heater usually enters the heater at lower pressure in cascade mode (LPH-3 and 4, HPH-6 and 7), or enters the drip pump (LPH-2 2) or a lower pressure reservoir (LPH-1 and HPH-5).

Fig. 3 shows the T-S diagram of the power plant cycle. In this diagram, the condensation processes for steam in each heater are clearly visible. Additionally, the diagram presents the pressure of input steam entering each heater.

To evaluate the overall effect of each group of pre-heaters (LP and HP) while removing them from the service in the software, the results are presented in Table 4. The following parameters are studied: energy and exergy efficiencies ( $\eta_1$ ,  $\eta_2$ ), fuel mass flow rate ( $\dot{m}_{fuel}$ ), water temperature difference in cooling tower ( $\Delta T_{CT}$ ), FW temperature to the econ-

omizer ( $T_{Econ}$ ) and equivalent production power ( $P$ ). These parameters were calculated for 4 modes, and the heaters in service are LPHs, HPHs, LPHs+HPHs and without heaters. As it is shown, if all of the heaters are out of service,  $\eta_1$ , and  $\eta_2$  become 32.02% and 31.25%, which is 3.19% and 3.1% lower, respectively, than is case with all heaters working. It is worth noting that in some cases, because of repairs to the power plant or leakage from the heaters (internal or external), this equipment should be removed from service. Deciding whether to use a unit in this situation or to shut it down and perform repairs requires sufficient information about unit efficiency and power generation priority (networks need) among other parameters.

One issue that may arise for heaters is a change in FW temperature rise. This change (usually a reduction) may occur due to increased heat transfer resistance owing to: (i) the formation of sediment on the heat transfer surfaces, (ii) steam valve breakdown (wear and tear of internal parts) or (iii) reduction of unit power production [21]. In addition, these pipes can be blocked from both sides if there is an internal leak in the tubes inside the heater and there is only a small number of tubes. The heater will continue to operate (for a short time), but the heat exchange rate will deteriorate and eventually the temperature rise of the FW will slow down [21]. In Fig. 4, changes in the exergy efficiency of the LP heaters are observed against the change in temperature rise in these heaters.

Increasing the  $\Delta T$  of the heater results in increased functional exergy efficiency ( $\eta_{2,f}$ ). In contrast, increasing  $\Delta T$  results in reducing universal exergy efficiency ( $\eta_{2,u}$ ). This contradiction is due to the difference in the definition of these efficiencies (Equations 10 and 11). As shown in Fig. 4, the trend of  $\eta_{2,f}$  is increasing and has no peak point. Higher  $\Delta T$  results in higher  $\eta_{2,f}$ . On the other hand,  $\eta_{2,u}$  trend is increasing and almost all of the charts have a minimum point. Fig. 5 depicts variations of  $\eta_{2,f}$  and  $\eta_{2,u}$  vs.  $\Delta T$  of HP heaters. The general trend of these parameters in HP heaters is similar to that of LP heaters. The only difference is for HPH-5, in which, unlike other heaters,  $\eta_{2,u}$  does not have a minimum point, and higher  $\Delta T$  results in lower  $\eta_{2,u}$ .

In order to compare the exergy efficiencies of all heaters with each other, Figs. 6 and 7 show  $\eta_{2,u}$  and  $\eta_{2,f}$  for all heaters. As shown in Fig. 6, in a particular  $\Delta T$ , there is a significant difference between the universal exergy efficiencies of heaters. Examining this chart, it can be concluded that lowering FW temperature results in lower universal exergy efficiency. Also, lowering FW temperature results in higher variation of heater exergy efficiency. From Fig. 6 it is observed that as  $\Delta T$  approaches zero, the universal exergy efficiency approaches 100%.

Fig. 7 shows the variations of functional exergy efficiency ( $\eta_{2,f}$ ) vs  $\Delta T$  of all heaters. This diagram is similar to Fig. 6 because for a particular  $\Delta T$ , lowering the temperature of the FW in the heater results in lowering the functional exergy efficiency. This can also be seen in Equations 10 and 11. The difference between this diagram and Fig. 6 is that at  $\Delta T = 0$ ,  $\eta_{2,f}$  approaches 0% (whilst  $\eta_{2,u}$  approaches 100%).

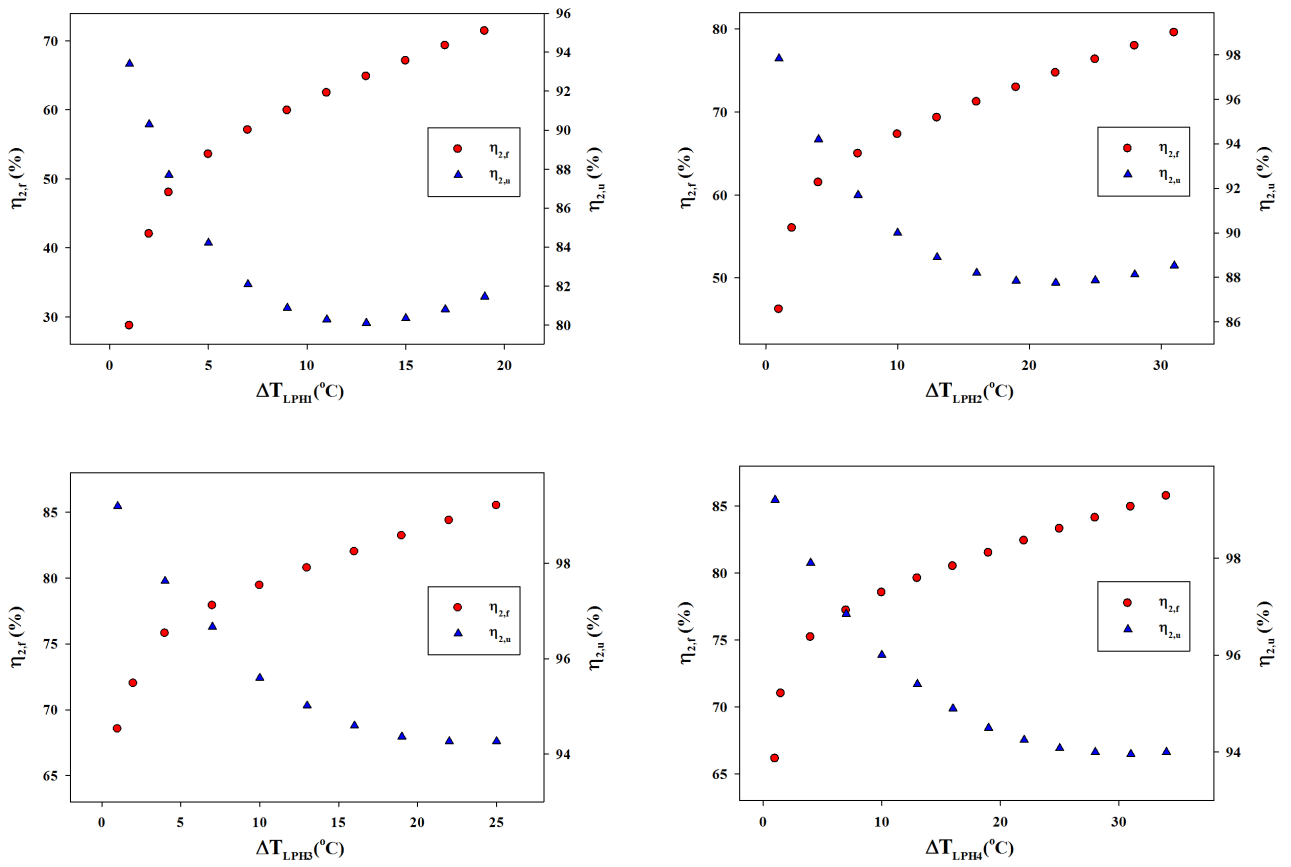


Figure 4: Variation of exergy efficiencies ( $\eta_{2,f}$  and  $\eta_{2,u}$ ) of LPHs vs. the variation of  $\Delta T_{LPHs}$

Fig. 8 shows variations in energy and exergy efficiencies ( $\eta_1$  and  $\eta_2$ ) of the cycles vs.  $\Delta T$  of heaters. As can be seen, increasing  $\Delta T$  results in increased energy and exergy efficiencies. In the case where all heaters are fully in service,  $\eta_1$  and  $\eta_2$  are 35.21% and 34.35%. Comparing the diagrams in Fig. 8, it can be concluded that the variations of both efficiencies are similar. In addition, examining each of these graphs, it can be seen that LPH-2 has the greatest effect on increasing the cycle efficiencies. In this regard, LPH-1 is ranked second.

One of the beneficial effects of FWHs in the Rankine cycle is the consumption of a portion of the steam passing through the turbine. In this way, part of the steam entering the turbine will not enter the condenser. Although this will reduce the steam flow rate through the turbine in the final stages, the final result is beneficial. The condensation of steam in the condenser has two negative effects: first, the equipment needs to cool the cooling water (resulting in internal electricity consumption); secondly, the energy transferred to the cooling tower in the form of heat is released to the atmosphere and reduces the efficiency of the cycle [3]. In this section, with the assumption of constant mass flow rate of cooling water in the cooling tower and the assumption of the production of 200 MW, the variation in  $\Delta T_{CT}$  and  $\Delta T$  of each heater is shown in Fig. 9. This is one of the most important problems in some thermal power plants [5]. The rates shown in Fig. 9 are exactly the same as graphs of Fig. 8. Therefore LPH-2 results in the highest increase in  $\Delta T_{CT}$ . The minimum effect is obtained from HPH-5. The optimal heater (or heaters) are therefore selected for feed water heating repowering [10–14]. The goal is to have the least negative effect on power generation and minimize impact on cooling the tower cooling capacity.

Fig. 10 shows the effect of  $\Delta T$  of the HP heaters (individually) on the production power. To calculate the production power in Fig. 10, it is assumed that the fuel flow and hence the heat absorbed by the FW in the boiler is constant. Reducing  $\Delta T$  of the heater reduces the production power while the fuel flowrate is constant. In Fig. 9 it is also observed that the reduction of  $\Delta T$  of the heater caused an increase in the heat lost through the cooling tower. From Fig. 10, it can be concluded that HPH-6 has the greatest effect among all HP heaters.

Fig. 11 shows the effect of  $\Delta T$  of each heater on the heat absorbed for all heaters. The most significant change occurs for HPH-7 and the least change occurs for LPH-1. This shows that at a constant  $\Delta T$ , the higher the FW temperature in the heater, the higher the heat exchanged in the heater, and vice versa.

One of the main goals of this paper was to investigate the effects of leakage of condensate of heaters to the condenser. Normally, the condensate of the LP heaters (except LPH-1) is injected into the FW pipeline through the drip pump (at the point after LPH-2). Also, the condensate of HP heaters enters the deaerator (to optimize its energy use). But for both heater groups, a path to the condenser is also predicted. In the absence of a preconfigured path, the condensate of

heaters should be sent to the condenser. If there are internal leakages in valves on this path (internal leakage), due to the lower pressure of condenser side, part of the condensate enters the condenser. Due to the fact that the mass flow rate of condensate of LP and HP heaters are 17.79 and 22.01 kg/s, respectively, therefore their entry into the condenser can increase the cooling tower load and the power consumption of relevant pumps [5]. In addition, due to the lack of optimal use of these streams (energies), fuel consumption also increases (in other words, the output power decreases in the constant fuel flow).

In Fig. 12, changes in energy and exergy efficiencies of the cycle against the leaked mass flow rate of condensate of each group of heaters (LPHs and HPHs) to the condenser are shown. In addition, the leakage effect of both groups (LPHs+HPHs) was also studied. The efficiency of the cycle is reduced by increasing the leakage of drainage of the heaters into the condenser. Moreover, it can be concluded that the effect of HPHs is greater than LPHs. There are various reasons why the leaked condensate enters the condenser, some of which are temporary and inevitable. For example, when the drip pump is out of service, the condensate of LPHs is inserted into the condenser. Alternatively, because of problems in the deaerator (leakage along the way or in the valves), condensate of HPHs is sent to the condenser. However, one reason may be defects in the valve on the condenser pipeline. This occurs when there is erosion in the interior part of the valves or there are faults in the instrumentation section of the valves.

In Fig. 13, the effect of mass flow rate of leakage of the heat exchangers (all three conditions) on  $\Delta T_{CT}$  is observed. As already stated,  $\Delta T_{CT}$  value is obtained assuming that the mass flow rate of the coolant water is constant. Clearly, in a particular leakage flow rate, the leakage effect of HPHs is greater than that of LPHs, because the temperature of the outlet condensate from the HPH-5 is higher than LPH-2. This point can be clearly seen in Fig. 13. This figure shows that if there is a leakage of 20 kg/s from the pathway of the HPHs, the temperature difference between the cooling tower increases by about 0.18°C. For the same amount of leakage from the path to the LPHs, temperature difference becomes 0.09°C, which is much less than the temperature difference for HPHs.

Given the fact that the leakage of condensate to the condenser increases the losses in the cooling tower and reduces cycle efficiency, assuming that the power is constant, there is an increase in fuel consumption. Higher fuel consumption results in a higher rate of emissions of environmental pollutants. Fig. 14 shows the rate of increase of CO<sub>2</sub> production compared to the leakage rate of the heaters. Changes in Fig. 14 are similar to Fig. 13, which means that HPHs are more effective than LPHs. According to Fig. 14, if there is a leak of 20 kg/s from the pathway of the HPHs, the production of CO<sub>2</sub> will increase by 7200 ton/year.

## 6. Conclusions

In the present paper, the performance of FWHS of a steam power plant with a capacity of 200 MW was evaluated. The main objective of this study was to investigate the behavior of these heaters in various scenarios. The behavior of heaters and parameters affecting their performance were studied. In order to re-power old steam units, eliminating FWHS is effective for feed water heating re-powering and full re-powering [10]. In this study, all the FWHS were studied separately and collectively (LP, HP, and both groups) in different scenarios. Some of the results are exclusive to the studied power plant. These results depend on the dimensions and the thermodynamic parameters of heaters. Other results can be generalized to similar power plants. The effect of leakage of condensates (LP, HP, and both) on the condenser was also studied in detail.

General results of this paper include in particular:

1. For all heaters, higher exchanged heat (i.e.,  $\Delta T_{FW}$  increases) results in higher universal exergy efficiency and lower functional exergy efficiencies (in accordance with Equations 10 and 11).
2. HPH-7 and LPH-1 have the highest and lowest exergy efficiencies, which in normal operating conditions are 94.14% and 71.31%, respectively.
3. HPH-6 and LPH-1 have the highest and lowest rates of exergy destruction, which under normal operating conditions are 1039 and 397 kW, respectively.
4. Although the highest heat exchanges occur in HPH-6 and LPH-4 (31.3 and 21.73 MW), the highest positive effect on energy efficiency is due to LPH-2 and LPH-1 (0.81% and 0.61/0%).
5. In the event of a leak in condensate of heaters, the most negative effect is incurred by HP heaters. With a 20 kg/s leakage in each of these paths, the results are:
  - Reductions in energy efficiency of the cycle due to leakage in the LP and HP paths are 0.091% and 0.374%.
  - Reductions in produced power due to leakage in the LP and HP paths are 1.2 and 3.9 MW.
  - Annualized increases in CO<sub>2</sub> production due to leakage in the LP and HP paths are ca. 2300 and 7850 tons.
  - Leakage in the LP and HP paths results in increases in  $\Delta T_{CT}$  of 0.90 and 0.18°C.
  - Leakage in the LP and HP paths results in increases in internal consumption of 457 and 127 kW.
6. LPH-2 and LPH-1 have the greatest effect on  $\Delta T_{CT}$  (0.36 and 0.28°C).
7. Installing LP and HP heaters boosts energy efficiency by 2.53% and 0.82%.

## References

- [1] J. Blazquez, R. Fuentes-Bracamontes, C. A. Bollino, N. Nezamuddin, The renewable energy policy paradox, *Renewable and Sustainable Energy Reviews* 82 (2018) 1–5.
- [2] G. R. Ahmadi, D. Toghraie, Energy and exergy analysis of montazeri steam power plant in iran, *Renewable and Sustainable Energy Reviews* 56 (2016) 454–463.
- [3] S. L. Dixon, *Fluid Mechanics, Thermodynamics of Turbomachinery*, 7th Edition, Pergamon Press, 2014.
- [4] Iran detailed statistics of electricity industry, for strategic management, in Persian (accessed 4.10.2018) (2016). URL <http://amar.tavanir.org.ir>
- [5] A. R. Seifi, O. A. Akbari, A. A. Alrashed, F. Afshary, G. A. S. Shabani, R. Seifi, M. Goodarzi, F. Pourfatah, Effects of external wind breakers of heller dry cooling system in power plants, *Applied Thermal Engineering* 129 (2018) 1124–1134.
- [6] G. Ahmadi, O. A. Akbari, M. Zarringhalam, Energy and exergy analyses of partial re-powering of a natural gas-fired steam power plant, *International Journal of Exergy* 23 (2) (2017) 149–168.
- [7] S. N. Naserabad, A. Mehrpanahi, G. Ahmadi, Multi-objective optimization of hrsg configurations on the steam power plant re-powering specifications, *Energy* 159 (2018) 277–293.
- [8] G. Ahmadi, D. Toghraie, O. A. Akbari, Technical and environmental analysis of re-powering the existing chp system in a petrochemical plant: A case study, *Energy* 159 (2018) 937–949.
- [9] O. Akbari, A. Marzban, G. Ahmadi, Evaluation of supply boiler re-powering of an existing natural gas-fired steam power plant, *Applied Thermal Engineering* 124 (2017) 897–910.
- [10] G. R. Ahmadi, D. Toghraie, Parallel feed water heating re-powering of a 200 mw steam power plant, *Journal of Power Technologies* 95 (4) (2015) 288–301.
- [11] G. Ahmadi, D. Toghraie, A. Azimian, O. A. Akbari, Evaluation of synchronous execution of full re-powering and solar assisting in a 200 mw steam power plant, a case study, *Applied Thermal Engineering* 112 (2017) 111–123.
- [12] G. Ahmadi, O. A. Akbari, M. Zarringhalam, Energy and exergy analyses of partial re-powering of a natural gas-fired steam power plant, *International Journal of Exergy* 23 (2) (2017) 149–168.
- [13] G. Ahmadi, D. Toghraie, O. A. Akbari, Solar parallel feed water heating re-powering of a steam power plant: a case study in iran, *Renewable and Sustainable Energy Reviews* 77 (2017) 474–485.
- [14] G. Ahmadi, D. Toghraie, O. A. Akbari, Efficiency improvement of a steam power plant through solar re-powering, *International Journal of Exergy* 22 (2) (2017) 158–182.
- [15] G. P. Varma, T. Srinivas, Parametric analysis of steam flashing in a power plant using waste heat of cement factory, *Energy Procedia* 90 (2016) 99–106.
- [16] A. Pourshaghagh, The optimum pressure for working fluid in feed water heaters of steam power plants, *Energy Equipment and Systems* 4 (2) (2016) 245–253.
- [17] A. Moghadassi, F. Parvizian, B. Abareshi, F. Azari, I. Alhajri, Optimization of regenerative cycle with open feed water heater using genetic algorithms and neural networks, *Journal of Thermal Analysis and Calorimetry* 100 (3) (2010) 757–761.
- [18] S. Farhad, M. Saffar-Avval, M. Younessi-Sinaki, Efficient design of feedwater heaters network in steam power plants using pinch technology and exergy analysis, *International journal of energy research* 32 (1) (2008) 1–11.
- [19] H. D. Akolekara, P. Srinivasan, J. Challa, Development of a simulation program to optimise process parameters of steam power cycles, *International Journal of Thermal & Environmental Engineering* 8 (1) (2014) 55–61.
- [20] L. Jiping, H. Wei, W. Xin, H. Xiaoku, C. Daotong, Y. Junjie, Theoretical investigation on the partial load feedwater heating system with thermal vapor compressor in a coal-fired power unit, *Energy Procedia* 75 (2015) 1102–1107.
- [21] M. A. Antar, S. M. Zubair, The impact of fouling on performance evaluation of multi-zone feedwater heaters, *Applied Thermal Engineering* 27 (14-15) (2007) 2505–2513.
- [22] J.-q. Xu, T. Yang, Y.-y. Sun, K.-y. Zhou, Y.-f. Shi, Research on vary-

- ing condition characteristic of feedwater heater considering liquid level, Applied Thermal Engineering 67 (1-2) (2014) 179–189.
- [23] M. Álvarez-Fernández, L. del Portillo-Valdés, C. Alonso-Tristán, Thermal analysis of closed feedwater heaters in nuclear power plants, Applied Thermal Engineering 68 (1-2) (2014) 45–58.
- [24] S. Espatolero, L. M. Romeo, C. Cortés, Efficiency improvement strategies for the feedwater heaters network designing in supercritical coal-fired power plants, Applied Thermal Engineering 73 (1) (2014) 449–460.
- [25] S. Hossienalipour, S. Karbalaee, H. Fathiannasab, Development of a model to evaluate the water level impact on drain cooling in horizontal high pressure feedwater heaters, Applied Thermal Engineering 110 (2017) 590–600.
- [26] C. Goujon, T. Pauporté, A. Bescond, C. Mansour, S. Delaunay, J.-L. Bretelle, Effects of curative and preventive chemical cleaning processes on fouled steam generator tubes in nuclear power plants, Nuclear Engineering and Design 323 (2017) 120–132.
- [27] I. E. Cáceres, R. M. Montañés, L. O. Nord, Flexible operation of combined cycle gas turbine power plants with supplementary firing, Journal of Power Technologies 98 (2) (2018) 188–197.
- [28] M. A. Gonzalez-Salazar, T. Kirsten, L. Prchlik, Review of the operational flexibility and emissions of gas-and coal-fired power plants in a future with growing renewables, Renewable and Sustainable Energy Reviews 82 (1) (2018) 1497–1513.
- [29] Archive of Isfahan Mohammad Montazeri Power Station in Iran. URL <http://en.persian-holding.ir/MMPowerplant>
- [30] Department of Environment, Islamic Republic of Iran, accessed 4.10.2018. URL <https://en.doe.ir/Portal/Home/default.aspx>
- [31] C. Borgnakke, E. Richard, Fundamentals of thermodynamics, John Wiley & Sons, Inc, United States, 2009.
- [32] I. Dincer, M. A. Rosen, Exergy: energy, environment and sustainable development, Newnes, 2012.
- [33] M. Ameri, P. Ahmadi, A. Hamidi, Energy, exergy and exergoeconomic analysis of a steam power plant: A case study, International Journal of Energy Research 33 (5) (2009) 499–512.
- [34] S. N. Naserabad, K. Mobini, A. Mehrpanahi, M. Aligoodarz, Exergy-energy analysis of full repowering of a steam power plant, Frontiers in Energy 9 (1) (2015) 54–67.
- [35] TU Delft, Postbus, Delft, The Netherlands, Cycle-Tempo Manual, "Technical notes", Cycle-Tempo release 5.0- A program for thermodynamic modeling and optimization of energy conversion systems (2017).

## Nomenclature

### Abbreviations

GC Gland condenser  
 GTCC Gas turbine combined cycle  
 HPH High-pressure heater  
 HPT High-pressure turbine  
 IPT Intermediate-pressure turbine  
 LP Low pressure  
 LPH Low-pressure heater  
 MSPP Montazeri steam power plant  
 Pre Preheater  
 RC Rankine cycle  
 BFP Boiler feed pump

SC Simple cycle  
 SPP Steam power plant  
 ST Steam turbine  
 CWP Cooling water pump  
 CCGP Combined cycle power plant  
 DE Deaerator  
 Econ Economizer  
 Evap Evaporator  
 FW Feed water  
 FWH Feed water pre-heater  
 GSC Gland steam cooler  
 Greek Symbols  
 $\eta_1$  First low efficiency  
 $\eta_2$  Second low efficiency  
 $\eta_{2,f}$  Functional exergy efficiency  
 $\eta_{2,u}$  Universal exergy efficiency  
 $\xi$  Exergy of fuels  
 $\psi$  Specific exergy, kW/kg  
 Parameters  
 $\Delta T$  Temperature difference, °C  
 P Pressure, bar  
 Q Heat, kW  
 $\bar{R}$  World constant for gases  
 s Specific entropy, kJ/kgK  
 T Temperature, °C  
 v Velocity, m/s  
 W Work, kW  
 e Specific energy, kJ/kg  
 E Total energy, kJ  
 EX Flow exergy  
 g The gravity acceleration, m/s<sup>2</sup>  
 h Specific enthalpy, kJ/kg  
 HR Heat rate, kJ/kg  
 $\dot{i}$  Destroyed exergy, kW  
 $\dot{m}$  Mass flow rate, kg/s

Subscripts and superscripts

des destroyed

f fuel

gen generated

i inlet

l lost

o outlet

p primary

s secondary

Table 3: Properties of FWHs

heater	$T_{FW}, ^\circ\text{C}$		Steam		$\Delta P_{FW}, \text{bar}$		Steam cooler	Drain cooler	Q, MW	$\Delta T_{FW}, ^\circ\text{C}$
	inlet	outlet	T, $^\circ\text{C}$	P, bar	$\Delta P_{FW}, \text{bar}$	bar				
LPH-1	48.2	68.6	71.79	0.337	1.5	1.5	—	—	10.2	18.9
LPH-2	72.71	102.2	182.1	1.25	2	2	—	—	16.02	29.5
LPH-3	102.7	126.1	260.2	5.63	1.5	1.5	—	√	14.84	23.4
LPH-4	126.1	159.9	353.7	5.98	1.5	1.5	√	—	21.73	33.8
Deae	159.9	165.5	432.9	7.04	0	0	—	—	3.38	5.6
HPH-5	168.2	183.2	432.9	11.29	2	2	√	√	11.34	15
HPH-6	183.2	223.3	351.5	25.3	2	2	√	√	31.1	40.1
HPH-7	223.3	244.9	395.5	36.74	2	2	√	√	17.37	21.6

Table 4: Effect of FWHS on power plant performance

Working Heaters	$\eta_1$	$\eta_2$	$\dot{m}_{fuel}$ , kg/s	$P_i$ , MW	$\Delta T_{CT}$ , °C	$T_{ECON}$ , °C
LPHs	34.39	33.55	12	194.5	10.46	168
HPHs	32.68	31.88	12.63	186	11.38	159
LPHs+HPHs	35.21	34.35	11.7	200	10	244.6
None	32.02	31.25	12.91	181.5	11.78	83

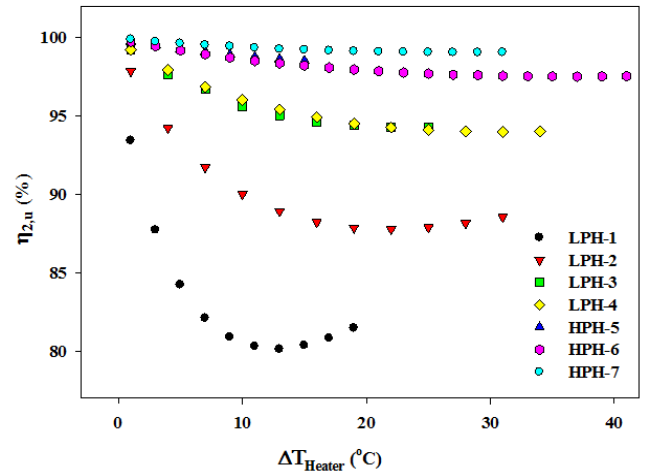
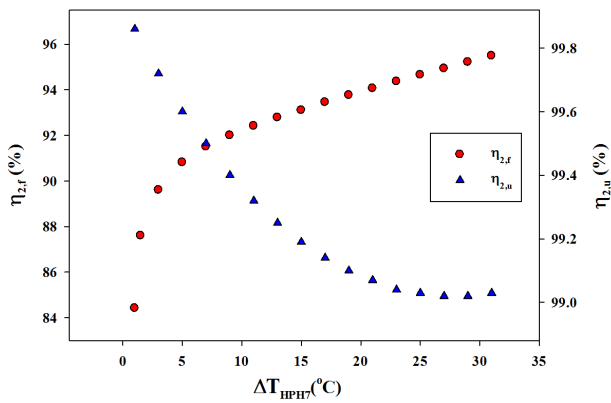
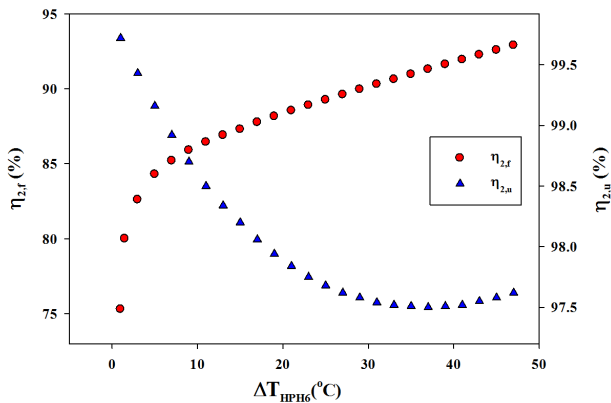
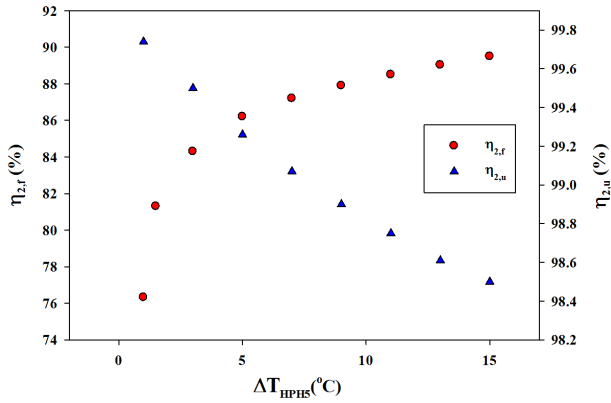


Figure 6: Comparison of  $\eta_{2,u}$  for all heaters

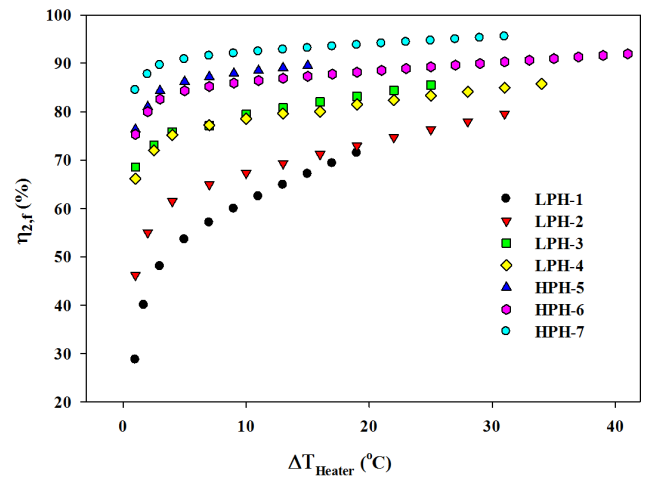


Figure 7: Comparison of  $\eta_{2,f}$  for all heaters

Figure 5: Variation of exergy efficiencies ( $\eta_{2,f}$  and  $\eta_{2,u}$ ) of HPHs vs. variation of  $\Delta T_{HPHs}$

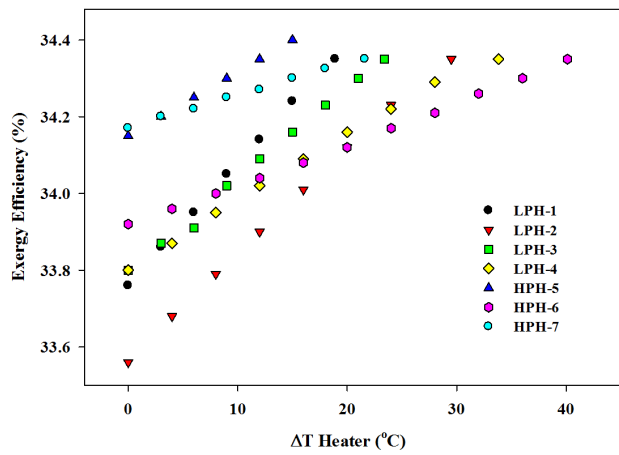
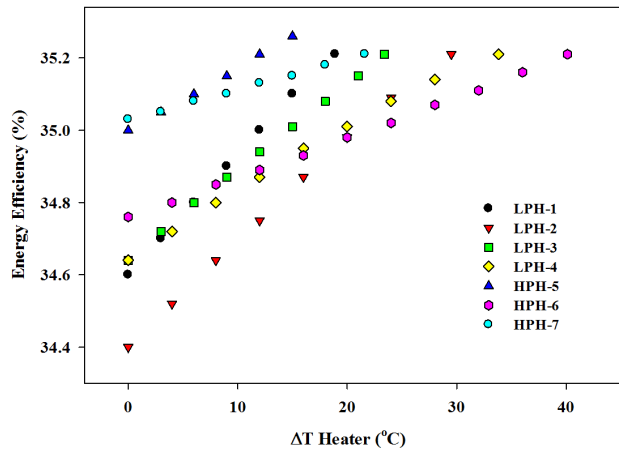


Figure 8: Variation of energy and exergy efficiencies of the cycle vs. variation of  $\Delta T_{Heaters}$

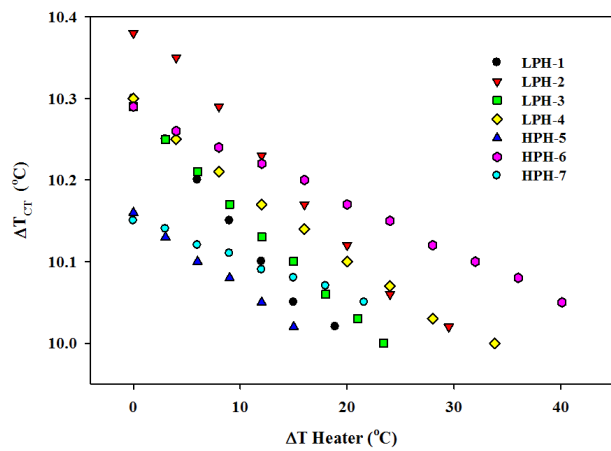


Figure 9: Variation of  $\Delta T_{CT}$  vs. variation of  $\Delta T_{Heaters}$

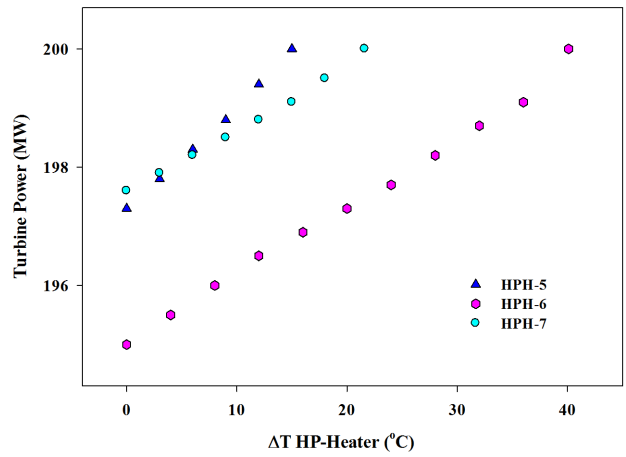


Figure 10: Variation of produced power vs. variation of  $\Delta T_{Heaters}$

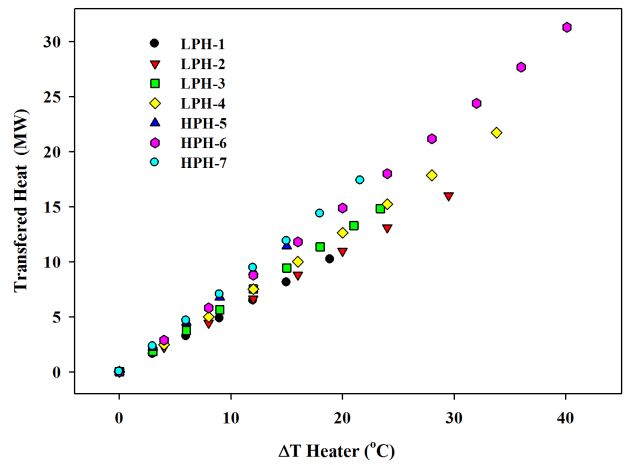


Figure 11: Variation of transmitted heat vs. variation of  $\Delta T_{Heaters}$

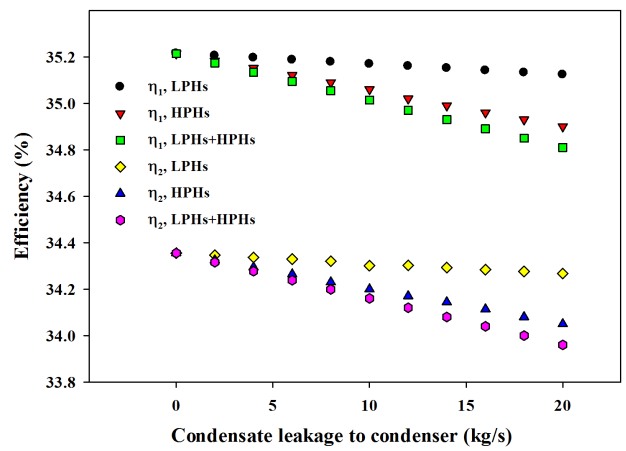


Figure 12: Variation of efficiencies vs. variation of mass flow rate of leakages (all groups)

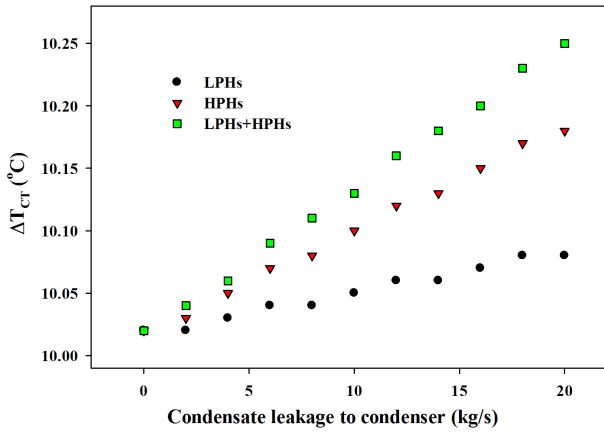


Figure 13: Variation of  $\Delta T_{CT}$  vs. variation of mass flow rate of leakages (all groups)

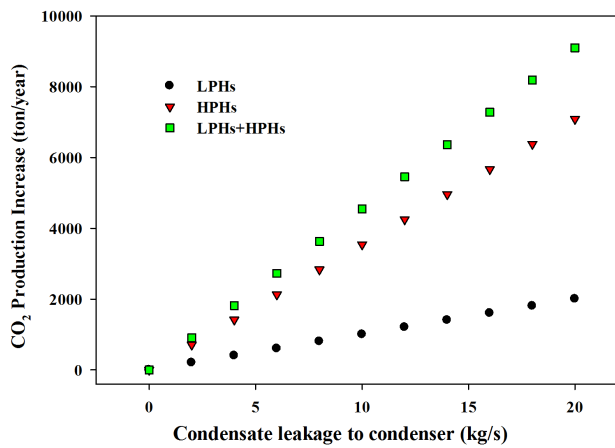


Figure 14: Variation of the rate of  $CO_2$  production vs. variation of mass flow rate of leakages (all groups)